

# Functional Nanoparticle-Based Proteomic Strategies for Characterization of Pathogenic Bacteria

Wei-Jen Chen,<sup>†</sup> Pei-Jane Tsai,<sup>‡</sup> and Yu-Chie Chen<sup>\*,†</sup>

Department of Applied Chemistry, National Chiao Tung University, Hsinchu 300, Taiwan, and National Laboratory Animal Center, National Applied Research Laboratories, Taipei 115, Taiwan

Although matrix-assisted laser desorption/ionization mass spectrometry (MALDI MS) can be employed to rapidly characterize pathogenic bacteria, bacterial cultures are generally required to obtain sufficient quantities of the bacterial cells prior to MALDI MS analysis. If this time-consuming step could be eliminated, the length of time required for identification of bacterial strains would be greatly reduced. In this paper, we propose an effective means of rapidly identifying bacteria—one that does not require bacterial culturing—using functional nanoparticle-based proteomic strategies that are characterized by extremely short analysis time. In this approach, we used titania-coated magnetic iron oxide nanoparticles ( $\text{Fe}_3\text{O}_4@\text{TiO}_2$  NPs) as affinity probes to concentrate the target bacteria. The magnetic properties of the  $\text{Fe}_3\text{O}_4@\text{TiO}_2$  NPs allow the conjugated target species to be rapidly isolated from the sample solutions under a magnetic field. Taking advantage of the absorption of the magnetic  $\text{Fe}_3\text{O}_4$  NPs in the microwave region of the electromagnetic spectrum, we performed the tryptic digestion of the captured bacteria under microwave heating for only 1–1.5 min prior to MALDI MS analysis. We identified the resulting biomarker ions by combining their MS/MS analysis results with protein database searches. Using this technique, we identified potential biomarker ions representing five Gram-negative bacteria: *Escherichia coli* O157:H7, uropathogenic *E. coli*, *Shigella sonnei*, *Pseudomonas aeruginosa*, and *Klebsiella pneumoniae*. Finally, we demonstrated the practical feasibility of using this approach to rapidly characterize bacteria in clinical samples.

Matrix-assisted laser desorption/ionization mass spectrometry (MALDI MS) can be employed to rapidly characterize microorganisms.<sup>1–11</sup> In addition, functional nanoparticles (NPs) can be

used as affinity probes for pathogenic bacteria.<sup>9–11,13–17</sup> Combining these techniques has led to the rapid characterization of pathogenic bacteria using MALDI MS after the bacteria have been concentrated using the affinity probes.<sup>1,2,9,11</sup> The affinity capture of bacteria in conjunction with MALDI MS analysis allows the detection of trace levels of bacteria with low interference from complex samples. In addition, proteomics strategies<sup>17,18</sup> can be employed to rapidly characterize target bacteria. For example, the biomarker ions obtained from tryptic digests of bacteria and their resultant MS/MS data can be matched to their parent proteins via protein database searching; the corresponding bacterial strains are then identified.

When employing MALDI MS to characterize bacteria, it is desirable for the affinity probes to have broad affinity toward bacteria. Lectins,<sup>4–6</sup> immunoglobulin G,<sup>9,10</sup> and vancomycin,<sup>11,13–16</sup> which all have broad affinity for bacteria, have been immobilized onto the surfaces of affinity probes. Magnetic NPs coated with metal oxides, such as titanium oxide,<sup>19–21</sup> zirconium oxide,<sup>22,23</sup>

- (4) Bundy, J.; Fenselau, C. *Anal. Chem.* **1999**, *71*, 1460–1463.
- (5) Bundy, J.; Fenselau, C. *Anal. Chem.* **2001**, *73*, 751–757.
- (6) Afonso, C.; Fenselau, C. *Anal. Chem.* **2003**, *75*, 694–697.
- (7) Pribil, P.; Fenselau, C. *Anal. Chem.* **2005**, *77*, 6092–6095.
- (8) Hsieh, S.-Y.; Tseng, C.-L.; Lee, Y.-S.; Kuo, A.-J.; Sun, C.-F.; Lin, Y.-H.; Chen, J.-K. *Mol. Cell. Proteomics* **2008**, *7*, 448–456.
- (9) Ho, K.-C.; Tsai, P.-J.; Lin, Y.-S.; Chen, Y.-C. *Anal. Chem.* **2004**, *76*, 7162–7268.
- (10) Chen, W.-J.; Tsai, P.-J.; Chen, Y.-C. *Small* **2008**, *4*, 485–491.
- (11) Lin, Y.-S.; Tsai, P.-J.; Weng, M.-F.; Chen, Y.-C. *Anal. Chem.* **2005**, *77*, 1753–1760.
- (12) Russell, S. C.; Edwards, N.; Fenselau, C. *Anal. Chem.* **2007**, *79*, 5399–5406.
- (13) Gao, J.; Li, L.; Ho, P.-L.; Mak, G. C.; Gu, H.; Xu, B. *Adv. Mater.* **2006**, *18*, 3145–3148.
- (14) Gu, H. W.; Ho, P. L.; Tsang, K. W. T.; Wang, L.; Xu, B. *J. Am. Chem. Soc.* **2003**, *125*, 15702–15703.
- (15) Gu, H. W.; Ho, P. L.; Tsang, K. W. T.; Yu, C. W.; Xu, B. *Chem. Commun.* **2003**, *15*, 1966–1967.
- (16) Huang, W.-C.; Tsai, P.-J.; Chen, Y.-C. *Nanomedicine* **2007**, *2*, 777–787.
- (17) Fenselau, C.; Russell, S.; Swatkoski, S.; Edwards, N. *Eur. J. Mass Spectrom.* **2007**, *13*, 35–39.
- (18) Hettick, J. M.; Kashon, M. L.; Simpson, J. P.; Siegel, P. D.; Mazurek, G. H.; Weissman, D. N. *Anal. Chem.* **2004**, *76*, 5769–5776.
- (19) Chen, C.-T.; Chen, Y.-C. *Anal. Chem.* **2005**, *77*, 5912–5919.
- (20) Liang, X. Q.; Fonnum, G.; Hajivandi, M.; Stene, T.; Kjus, N. H.; Ragnhildstveit, E.; Arnshey, J. W.; Predki, P.; Pope, R. M. *J. Am. Soc. Mass Spectrom.* **2007**, *18*, 1932–1944.
- (21) Chen, C.-T.; Chen, Y.-C. *J. Biomed. Nanotechnol.* **2008**, *4*, 73–79.
- (22) Lo, C.-Y.; Chen, W.-Y.; Chen, C.-T.; Chen, Y.-C. *J. Proteome Res.* **2007**, *6*, 887–893.
- (23) Li, Y.; Leng, T. H.; Lin, H. Q.; Deng, C. H.; Xu, X. Q.; Yao, N.; Yang, P. Y.; Zhang, X. M. *J. Proteome Res.* **2007**, *6*, 4498–4510.

\* To whom correspondence should be addressed. E-mail: yuchie@mail.nctu.edu.tw. Fax: 886-3-5131527. Phone: 886-3-5131527.

<sup>†</sup> National Chiao Tung University.

<sup>‡</sup> National Applied Research Laboratories.

(1) Madonna, A. J.; Cuyk, S. V.; Voorhees, K. J. *Rapid Commun. Mass Spectrom.* **2003**, *17*, 257–263.

(2) Madonna, A. J.; Basile, F.; Furlong, E.; Voorhees, K. J. *Rapid Commun. Mass Spectrom.* **2001**, *15*, 1068–1074.

(3) Rees, J. C.; Voorhees, K. J. *Rapid Commun. Mass Spectrom.* **2005**, *19*, 2757–2761.

and aluminum oxide,<sup>24–26</sup> are effective affinity probes for phosphorylated species, which bind to the metal oxide surfaces through monodentate, bidentate, and tridentate interactions of the phosphate units to the metal ion centers.<sup>27</sup> Lipopolysaccharide (LPS), which comprises lipid A, a core oligosaccharide, and a distal polysaccharide, is a major component of the outer membrane of Gram-negative bacteria.<sup>28</sup> Apart from *Listeria monocytogenes*,<sup>29</sup> most Gram-positive bacteria lack the LPS-like structure; thus, Gram-positive bacteria interact only weakly with metal oxide-coated magnetic NPs. Because lipid A possesses phosphate units, we suspected that metal oxide-coated magnetic NPs would interact with bacteria presenting LPS via metal–phosphate chelation. If so, it would be possible to employ magnetic NPs coated with metal oxides to extract traces of target bacteria from complex samples.

Previous reports have described the combination of microwave-assisted bacterial digestions and mass spectrometric analyses.<sup>12,30</sup> Recently, we demonstrated the use of functional magnetic iron oxide NPs as affinity probes and microwave absorbers that assist in the extraction<sup>31</sup> and tryptic digestion<sup>32</sup> of biomolecules under microwave heating for 30–90 s. Using this concept, in this study we performed trapping experiments using magnetic iron oxide NPs coated with titania (Fe<sub>3</sub>O<sub>4</sub>@TiO<sub>2</sub> NPs) as affinity probes to target bacteria under microwave heating for 1.5 min. Subsequently, we performed tryptic digestion of the trapped bacterial cells—after rinsing and adding trypsin—under microwave heating for 1 min. To demonstrate the feasibility of this approach, we selected the common pathogens *Escherichia coli* O157:H7, *Shigella sonnei*, *Pseudomonas aeruginosa*, and *Klebsiella pneumoniae* as suitable bacterial samples. *S. sonnei* and *E. coli* O157:H7 can cause bloody diarrhea; *P. aeruginosa* and *K. pneumoniae* infections may result in pneumonia. Urinary tract infections (UTI) are most commonly caused by *E. coli*, although *P. aeruginosa* and *K. pneumoniae* may also cause them. We first used the proposed proteomic strategy to identify potential biomarkers of these bacterial strains and then demonstrated the possibility of using this approach to rapidly identify the presence of these bacteria in clinical bacterial samples.

## EXPERIMENTAL SECTION

**Reagents and Materials.** Iron(III) chloride hexahydrate, phosphoric acid, and ammonium bicarbonate were purchased from Riedel-de Haën (Seelze, Germany). Iron(II) chloride tetrahydrate, ammonium hydroxide solution, tetraethyl orthosilicate (TEOS), and nitric acid were purchased from Fluka (Steinheim, Germany). Ethanol was obtained from Showa (Tokyo, Japan). Trifluoroacetic acid (TFA) was obtained from Merck. Isopropyl alcohol, hydrochloric acid, and 2-propanol were obtained from J. T. Baker (Lane Phillipsburg, NJ). Titanium(IV) isopropoxide, LPS (isolated from *E. coli* O55:B5) and trypsin (from bovine pancreas)

were purchased from Sigma (St. Louis, MO). 2,5-Dihydroxybenzoic acid (DHB) and  $\alpha$ -cyano-4-hydroxycinnamic acid (CHCA) were purchased from Aldrich (Milwaukee, WI). Urine (pH ~6.7) was collected from healthy volunteers. Tryptic soy broth (TSB), Luria–Bertani (LB), and granulated agar were obtained from Becton Dickinson (Sparks, MD). Yeast extract was purchased from Alpha Bioscience (Baltimore, MD).

**Preparation of Titania-Coated Magnetic Iron Oxide Nanoparticles.** The titania-coated magnetic iron oxide nanoparticles were prepared using a previously described method.<sup>10</sup> The magnetic NPs were first prepared via coprecipitation. FeCl<sub>3</sub> (5.4 g) and FeCl<sub>2</sub> (2.0 g) were dissolved in aqueous hydrochloric acid (2 M, 25 mL) in a flask at room temperature under sonication. After the salts had dissolved completely, the flask was degassed using a vacuum pump and then it was filled with nitrogen gas. The contents of the flask were stirred for 10 min before aqueous ammonia (28%, 40 mL) was injected slowly over 1 h into the mixture under nitrogen while stirring at room temperature. The resulting solid was rinsed with deionized water (3 × 30 mL) and resuspended in deionized water (40 mL). The iron oxide NPs (0.2 g) obtained were rinsed with ethanol several times and then resuspended in ethanol (40 mL) under sonication for 1 h. Ammonia (4.5 mL), deionized water (3.75 mL), and TEOS (0.1 mL) were added sequentially to the NP suspension, which was then sonicated for 1 h and vortex-mixed for another 8 h. The silica-modified NPs were isolated through magnetic separation, and then they were rinsed with ethanol two or three times. The NPs were resuspended in ethanol (40 mL) and then heated under reflux at 60 °C for 12 h. After rinsing with deionized water, the generated NPs were resuspended in deionized water (40 mL). The suspension was acidified by adding a solution prepared from nitric acid (0.5 M, 0.22 mL) and deionized water (124.78 mL). The suspension was heated under reflux at 60 °C, and then a solution containing titanium isopropoxide (20  $\mu$ L) and 2-propanol (11.98 mL) was slowly injected into the mixture under stirring for 6 h. Because both TEOS and titanium isopropoxide are toxic, they should be handled with care by preparing the reagents in a hood and wearing gloves. The generated magnetic Fe<sub>3</sub>O<sub>4</sub>@TiO<sub>2</sub> NPs were rinsed twice with deionized water and resuspended in deionized water (40 mL) prior to use. Direct contact of the NPs on the skin should be avoided because they possess photocatalytic activity.

**Preparation of Bacterial Samples.** *E. coli* O157:H7, *E. coli* UTI, *S. sonnei*, *P. aeruginosa*, *K. pneumoniae*, *L. monocytogenes*, *Staphylococcus aureus*, and *Staphylococcus saprophyticus* were collected from patients at the General Tzu-Chi Hospital, Hualien, Taiwan. When preparing bacterial samples, it should be handled in a Biosafety Level 2 (BSL-2) laboratory. *L. monocytogenes*, *S. sonnei*, *P. aeruginosa*, and *K. pneumoniae* were cultured in TSBY (5 mL), which was prepared by dissolving TSB (24 g) and yeast (4 g) in deionized water (800 mL). *E. coli* O157:H7, *S. aureus*, *S. saprophyticus*, and *E. coli* UTI were cultured in LB broth (5 mL), which was prepared by dissolving LB (20 g) in deionized water (800 mL). After incubation for ~4 h at 37 °C, when the optical density (OD) of the bacterial sample solution reached 1, portions (200  $\mu$ L) of the bacterial solutions were added to fresh TSBY (or LB broth) (30 mL) and cultured for 24 h. The bacterial cells were then isolated through centrifugation (6000 rpm, 10 min) and rinsed with sterilized water (3 × 30 mL). The bacterial cell suspension

(24) Chen, C.-T.; Chen, W.-Y.; Tsai, P.-J.; Chien, K.-Y.; Yu, J.-S.; Chen, Y.-C. *J. Proteome Res.* **2007**, *6*, 316–325.

(25) Chen, C.-T.; Chen, Y.-C. *J. Mass Spectrom.* **2008**, *43*, 538–541.

(26) Chen, C.-T.; Chen, Y.-C. *J. Biomed. Nanotechnol.* **2008**, *4*, 73–79.

(27) Kirwan, L. J.; Fawell, P. D.; van Bronswijk, W. *Langmuir* **2003**, *19*, 5802–5807.

(28) Raetz, C. R. H.; Whitfield, C. *Annu. Rev. Biochem.* **2002**, *71*, 635–700.

(29) Wexler, H.; Oppenheim, J. D. *Infect. Immun.* **1979**, *23*, 845–857.

(30) Hu, A.; Chen, C.-T.; Tsai, P.-J.; Ho, Y.-P. *Anal. Chem.* **2006**, *78*, 5124–5133.

(31) Chen, W.-Y.; Chen, Y.-C. *Anal. Chem.* **2007**, *79*, 8061–8066.

(32) Chen, W.-Y.; Chen, Y.-C. *Anal. Chem.* **2007**, *79*, 2394–2401.

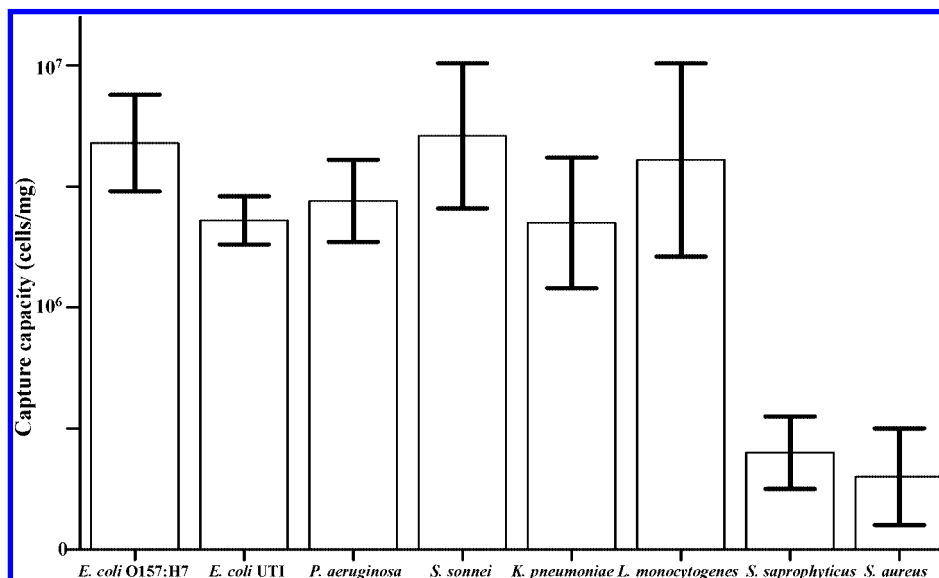
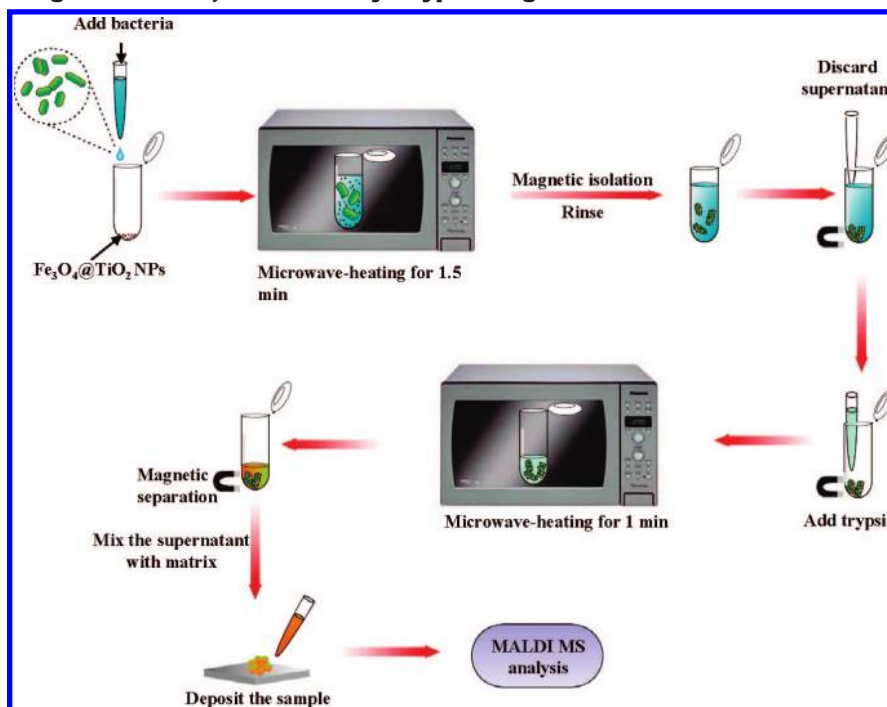


**Figure 1.** Bar graph of the capture capacity of  $\text{Fe}_3\text{O}_4@\text{TiO}_2$  NPs toward eight bacterial strains.

**Scheme 1. Cartoon Representation of the Process Employed When Using  $\text{Fe}_3\text{O}_4@\text{TiO}_2$  NPs To Selectively Trap Target Bacteria, Followed by Tryptic Digestion under Microwave Heating**



(1 mL) was heated in a water bath at 100 °C for 30 min. The bacterial cells were isolated through centrifugation (6000 rpm, 10 min), and then they were lyophilized for 24 h. The lyophilized cells were stored in a freezer (−20 °C) prior to use.

**Microwave-Assisted Trapping of LPS.** The trapping capacity of the  $\text{Fe}_3\text{O}_4@\text{TiO}_2$  NPs for LPS was examined using MALDI MS. For comparison,  $\text{Fe}_3\text{O}_4@\text{SiO}_2$  NPs were also employed as affinity probes toward bacteria.  $\text{Fe}_3\text{O}_4@\text{TiO}_2$  (or  $\text{Fe}_3\text{O}_4@\text{SiO}_2$ ) NPs (25  $\mu\text{g}$ ) were mixed with LPS (1  $\mu\text{g}/\text{mL}$ , 200  $\mu\text{L}$ ) by pipetting. The mixture was heated in a domestic microwave oven (900 W) for 1.5 min. The NP–target species conjugates were isolated through magnetic separation and rinsed several times with deionized water. The target species were eluted from the NPs by adding 2,5-DHB solution (15 mg/mL, 1  $\mu\text{L}$ ), which had been prepared in a mixture

of acetonitrile and deionized water (2:1, v/v) containing 1% phosphoric acid. The eluted solution was deposited on a MALDI sample plate. After evaporation of the solvent, the sample was ready for MALDI MS analysis.

**Estimation of Bacterial Trapping Capacity of  $\text{Fe}_3\text{O}_4@\text{TiO}_2$  NPs.** A bacterial sample (250  $\mu\text{L}$ ) was mixed with the  $\text{Fe}_3\text{O}_4@\text{TiO}_2$  NPs (625  $\mu\text{g}$ ) by pipetting. The mixture was placed in a domestic microwave oven (power, 900 W) and heated for 1.5 min. The NP–target species conjugates were isolated through magnetic separation. The trapping capacity of the NPs toward bacteria was estimated by measuring the OD (wavelength, 600 nm) of the remaining solution before and after magnetic trapping. Furthermore, to reduce the possibility of overestimating the trapping capacity, the isolated NP–bacterium conjugates were rinsed

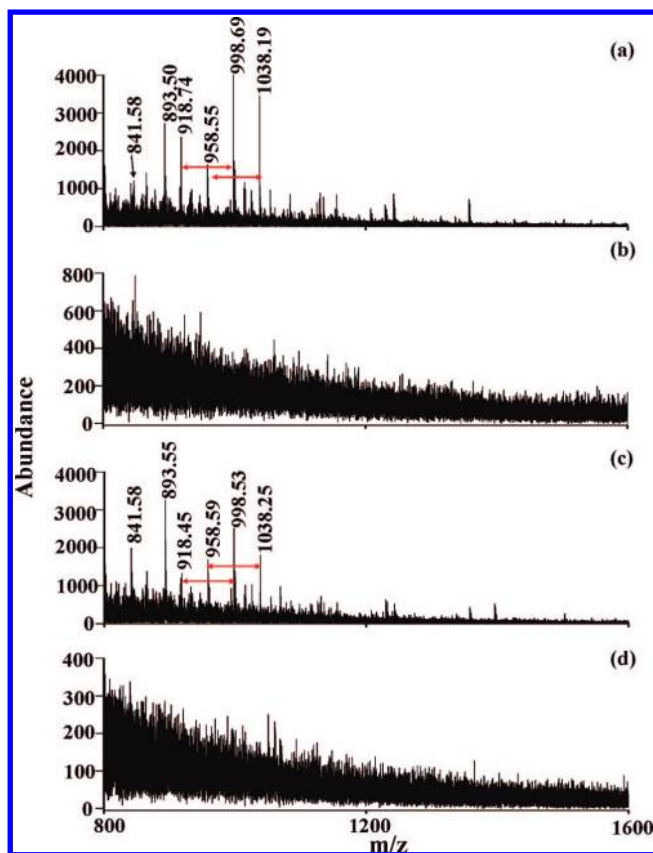


**Figure 2.** (a, b) Direct MALDI mass spectra of LPS at concentrations of (a) 100  $\mu\text{g/mL}$  (1  $\mu\text{L}$ ) and (b) 1  $\mu\text{g/mL}$  (1  $\mu\text{L}$ ). (c, d) MALDI mass spectra obtained after using (c)  $\text{Fe}_3\text{O}_4@\text{TiO}_2$  NPs (25  $\mu\text{g}$ ) and (d)  $\text{Fe}_3\text{O}_4@\text{SiO}_2$  NPs (25  $\mu\text{g}$ ) to trap their target species from LPS samples (1  $\mu\text{g/mL}$ , 200  $\mu\text{L}$ ). The MALDI matrix was 2,5-DHB (15 mg/mL, 1  $\mu\text{L}$ ) prepared in a mixture of acetonitrile and deionized water (2:1, v/v) containing 1% phosphoric acid.

repeatedly with deionized water (250  $\mu\text{L} \times 4$ ). The OD (wavelength, 600 nm) of the rinse solution was recorded and taken into consideration as nonspecific binding. The trapping capacity of the NPs toward bacteria was finally estimated by subtracting the degree of nonspecific binding. We then converted the final OD values to their corresponding cell concentrations (cells/mL) based on the calibration curve obtained by plotting the OD as a function of the cell concentration for each bacterial strain.

**$\text{Fe}_3\text{O}_4@\text{TiO}_2$  NP-Based Microwave-Assisted Capture and Tryptic Digestion of Bacteria.** Scheme 1 displays the steps involved when employing the  $\text{Fe}_3\text{O}_4@\text{TiO}_2$  NPs to capture target bacteria and then perform tryptic digestion under microwave heating. A bacterial sample solution (10  $\mu\text{L}$ ) was mixed with the  $\text{Fe}_3\text{O}_4@\text{TiO}_2$  NPs (25  $\mu\text{g}$ ) by pipetting, followed by heating in a microwave oven (power, 900 W) for 1.5 min. The cap of the sample vial was kept open during microwave heating. The NP–target species conjugates were isolated through magnetic separation and rinsed with deionized water. A solution of trypsin (18.75  $\mu\text{g/mL}$ , 1  $\mu\text{L}$ ) in ammonium hydrogencarbonate (50 mM) was added to the isolated conjugates. The mixture was incubated under microwave heating (power, 900 W) for 1 min. Then 1% TFA (0.2  $\mu\text{L}$ ) was added to the mixture to stop the digestion process. The sample was mixed with CHCA (25 mg/mL, 1  $\mu\text{L}$ ), and then the solution obtained from magnetic separation was deposited on a MALDI target for MALDI MS (or MS/MS) analysis. The amount

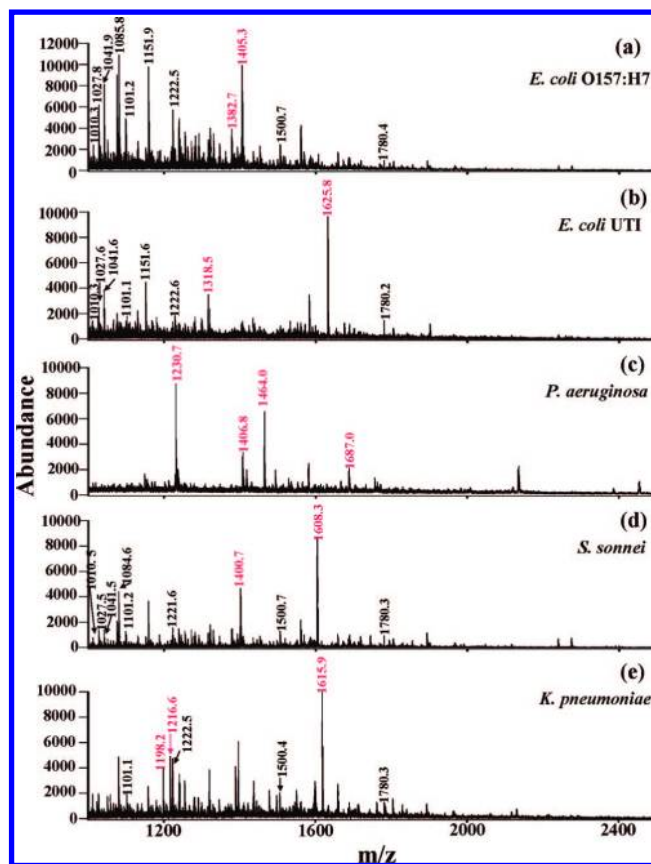


**Figure 3.** MALDI mass spectra obtained after using the  $\text{Fe}_3\text{O}_4@\text{TiO}_2$  NPs (25  $\mu\text{g}$ ) as affinity probes to trap target bacteria from aqueous samples (10  $\mu\text{L}$ ) containing (a) *E. coli* O157:H7 ( $1.85 \times 10^7$  cells/mL), (b) *E. coli* UTI ( $1.32 \times 10^7$  cells/mL), (c) *P. aeruginosa* ( $1.44 \times 10^7$  cells/mL), (d) *S. sonnei* ( $1.91 \times 10^7$  cells/mL), and (e) *K. pneumoniae* ( $1.83 \times 10^7$  cells/mL) under microwave heating (power, 900 W) for 1.5 min, followed by on-particle tryptic digestion under microwave heating (power, 900 W) for 1 min. CHCA (25 mg/mL, 1  $\mu\text{L}$ ) was the MALDI matrix.

of the NPs added in the bacterial solution, the cell concentration of bacteria, and the concentration of CHCA were varied to obtain optimized MALDI MS data. Mass spectra were calibrated using Bruker Daltonics peptide calibration reagents ( $M_w = 700\text{--}3200$  Da) as internal standards.

**Analysis of Clinical Bacterial Samples.** Three urine samples labeled A, B, and C containing *E. coli* UTI, *P. aeruginosa*, and *K. pneumoniae*, respectively, were collected from patients (the General Tzu-Chi Hospital, Hualien, Taiwan), who suffered from urinary tract infections. These urine samples were irradiated under UV light (254 nm) for 30 min in a BSL-2 laboratory before performing experiments. The urine samples (15  $\mu\text{L}$ ) were mixed with sterilized water (5  $\mu\text{L}$ ) and the  $\text{Fe}_3\text{O}_4@\text{TiO}_2$  NPs (25  $\mu\text{g}$ ). Bacteria in the samples were trapped by the  $\text{Fe}_3\text{O}_4@\text{TiO}_2$  NPs under microwave irradiation (power, 900 W) for 1.5 min. The cap of the sample vial was kept open during microwave heating. The NP–target species conjugates were isolated through magnetic separation and rinsed with sterilized deionized water (100  $\mu\text{L} \times 2$ ). A solution of trypsin (18.75  $\mu\text{g/mL}$ , 3  $\mu\text{L}$ ) in ammonium hydrogencarbonate (50 mM) was added to the isolated conjugates. The mixture was incubated under microwave heating (power, 900 W) for 1 min. Then 1% TFA (0.2  $\mu\text{L}$ ) was added to the mixture to stop the digestion process. The sample (2  $\mu\text{L}$ ) was mixed with

**Table 1. Peptides (m/z 1000–2500) Identified in the Analysis of Five Proteobacteria.**

MH <sup>+</sup>	MH <sub>calc</sub> <sup>+</sup>	peptide sequence	protein	<i>E. coli</i> O157:H7	<i>E. coli</i> UTI	<i>P. aeruginosa</i>	<i>S. sonnei</i>	<i>K. pneumoniae</i>
1010	1010.5	GHFFLHPR	amino acid antiporter probable glutamate/ γ-aminobutyrate antiporter	gi 15214333	gi 91210729			
1027	1027.6	AGENVGVLLR	acid sensitivity protein elongation factor Ef-Tu elongation factor Ef-Tu translation elongation factor Tu	gi 15834157 gi 168796536 gi 168714738	gi 162138356		gi 74312143 gi 74314474	
1041	1041.7	FSTALLHPR	lipid A biosynthesis lauroyl acyltransferase	gi 15830686	gi 91210205		gi 74311616	
1085	1085.5	RADKPSAGAGR	membrane-associated protein hypothetical protein putative outer membrane porin protein	gi 13361789 gi 168710436			gi 74312060	
1101	1101.5	QKGHAELYR	nitrogen regulatory protein P-II 2	gi 15829758	gi 91209524		gi 74311030	gi 3954959
1151	1151.6	MQFVMRLAR	putative minor tail protein	gi 15830090	gi 91214072			
1198	1198.3	HADNALTFGPR	50S ribosomal protein L6					gi 152972212
1216	1216.6	HHITADGFYR	50S ribosomal protein L32					gi 152969641
1222	1222.7	VVGQLGQVLGPR	50S ribosomal protein L1	gi 15834161	gi 122422147		gi 74314478	gi 152972841
1230	1230.6	RVEAEVEAEAK	major outer membrane protein OprF precursor			gi 4186419		
			outer membrane protein and related peptidoglycan- associated (lipo)proteins			gi 84321510		
1318	1318.7	MDITKILNTNR	putative phosphotransferase system (PTS), fructose- specific		gi 91213180			
1382	1382.7	GWLPPVCINPER	hypothetical protein	gi 15800725				
1400	1400.8	LDRDTSGVLLIAK	23S rRNA pseudouridylate synthase C				gi 74311647	
1405	1405.7	KVSLYLNNETPAG	hypothetical protein	gi 15831469				
1406	1406.9	DVLVNEYGVEGGR	major outer membrane protein OprF precursor			gi 4186419		
			outer membrane protein and related peptidoglycan- associated (lipo)proteins			gi 84321510		
1464	1463.8	IGFFNPVATGGVEVR	30S ribosomal protein S16			gi 14195196		
1500	1500.8	FAQKACSNIHILR	diaminopimelate decarboxylase	gi 15803358			gi 74313409	gi 152971771
1608	1607.8	YGFVASGTLNPQKAR	L-asparaginase II				gi 74313634	
1615	1615.8	SALPGSMVANVVADER	pullulanase D protein puID					gi 152968741 gi 7246031
1625	1625.8	MQFYSTPGAGAIRAR	hypothetical protein YfaP precursor		gi 91211519			
1687	1687.1	GVAMNPVDHPHGGGEGR	50S ribosomal protein L2 ribosomal protein L2			gi 42559303 gi 84318929		
1780	1780.4	MVVTLIHPIAMDDGLR	elongation factor Ef-Tu elongation factor Ef-Tu elongation factor Ef-Tu translation elongation factor Tu	gi 15834157 gi 168796536 gi 168736997	gi 162138356		gi 74314474	gi 152972232
					gi 91074389			

CHCA (25 mg/mL, 2 μL), and then the solution (1 μL) obtained from magnetic separation was deposited on a MALDI target for MALDI MS analysis.

**Database Searches.** Fragment peaks (S/N > 3) resulting from precursor ions (S/N > 3) were submitted via Biotools (v. 3.0) to MASCOT (www.matrixscience.com) using the following search parameters: the database searched was NCBI nr 20080616; taxonomy was limited to eubacteria; the enzyme was trypsin; MS and MS/MS tolerances were set at ±0.5 and ±0.8 Da, respectively; the number of missed cleavages was set to 1; the significance threshold was set at *p* < 0.05 because the score was over 50. Only one MS/MS spectrum resulting from a precursor ion was searched in the protein database search each time. Once identified, the peptide sequences were searched against the sequences of all proteins in the nonredundant protein sequence database using the basic local alignment search tool (BLAST; <http://www.ncbi.nlm.nih.gov/blast>).

**Instrumentation.** All absorption spectra were obtained using a Varian Cary 50 spectrophotometer (Melbourne, Australia). Mass spectra were obtained using a Bruker Daltonics Autoflex III TOF–TOF mass spectrometer. The following voltage parameters were employed: ion source 1, 19.06 kV; ion source 2, 16.61 kV; lens, 8.78 kV; reflector 1, 21.08 kV; reflector 2, 9.73 kV. The laser power was set to 45% with a frequency of 10 Hz, while each mass spectrum was collected from 500 laser shots. When MS/MS analyses were performed, the following voltage settings were used: ion source 1, 6.01 kV; ion source 2, 5.30 kV; lens, 3.01 kV; reflector 1, 27.10 kV; reflector 2, 11.74 kV; lift 1, 19.16 kV; lift 2, 4.42 kV. The laser power was set to 55% with a shot frequency of 10 Hz. Parent ions were obtained by collecting the mass spectra from 500 laser shots (50% power intensity) at a frequency of 10 Hz; daughter ions were obtained by collecting the mass spectra from 700 laser shots (70% power intensity) at a frequency of 10 Hz.

**Table 2. Proteins Identified in the Analysis of Five Gram-Negative Bacteria**

species	AC	protein	sequence coverage (%)	peptide sequence	MH <sub>obs</sub> <sup>+</sup>	Size (a.a)	score	
<i>E. coli</i> O157:H7	gi 15214333	probable glutamate/ γ-aminobutyrate antiporter	1	GHFFLHPR	1010.3	511	83	
	gi 168796536	elongation factor Ef-Tu	5	AGENVGVLLR	1027.8	186	105	
	gi 168736997	elongation factor Ef-Tu	4			241		
	gi 168714738	translation elongation factor Tu	3			286		
	gi 15834157	elongation factor Ef-Tu	2			394		
	gi 15830686	lipid A biosynthesis lauroyl acyltransferase	2	FSTALLHPR	1041.9	306	78	
	gi 13361789	membrane-associated protein	3	RADKPSAGAGR	1085.8	342	93	
	gi 168710436	hypothetical protein	3			336		
	gi 15829758	nitrogen regulatory protein P-II 2	8	QKGHAELYR	1101.2	112	86	
	gi 15830090	putative minor tail protein	8	MQFVMRLAR	1151.9	109	89	
	gi 15834161	50S ribosomal protein L1	5	VVGQLGQVLGPR	1222.5	234	83	
	gi 15800725	hypothetical protein	5	GWLPPVCINPER	1382.7	212	109	
	gi 15831469	hypothetical protein	20	KVSLYLNNETPAG	1405.3	62	113	
	gi 15803358	diaminopimelate decarboxylase	3	FAQKACSNHILR	1500.7	420	88	
	gi 168796536	elongation factor Ef-Tu	8	MVVTLIHPIAMDDGLR	1780.4	186	89	
	gi 168736997	elongation factor Ef-Tu	6			241		
	gi 15834157	elongation factor Ef-Tu	4			394		
	<i>E. coli</i> UTI	gi 91210729	amino acid antiporter	1	GHFFLHPR	1010.3	511	75
		gi 162138356	elongation factor Ef-Tu	2	AGENVGVLLR	1027.6	394	84
		gi 91074389	translation elongation factor Tu	2			409	
		gi 91210205	lipid A biosynthesis lauroyl acyltransferase	2	FSTALLHPR	1041.6	327	77
		gi 91209524	nitrogen regulatory protein P-II 2	8	QKGHAELYR	1101.1	112	82
		gi 91214072	putative minor tail protein	8	MQFVMRLAR	1151.6	109	83
gi 122422147		50S ribosomal protein L1	5	VVGQLGQVLGPR	1222.6	234	86	
gi 91213180		putative phosphotransferase system (PTS), fructose-specific	7	MDITKILNTNR	1318.5	156	104	
gi 91211519		hypothetical protein YfaP precursor	5	MQFYSTPGAGAIRAR	1625.8	258	108	
gi 162138356		elongation factor Ef-Tu	4	MVVTLIHPIAMDDGLR	1780.2	394	115	
gi 91074389		translation elongation factor Tu	3			409		
<i>P. aeruginosa</i>		gi 84321510	outer membrane protein and related peptidoglycan-associated (lipo)proteins	3			350	
		gi 4186419	major outer membrane protein OprF precursor	3			350	
	gi 84321510	outer membrane protein and related peptidoglycan-associated (lipo)proteins	4	DVLVNEYGVEGGR	1406.8	331	149	
	gi 4186419	major outer membrane protein OprF precursor	4			350		
	gi 14195196	30S ribosomal protein S16	16	IGFFNPVATGGEVR	1464.0	83	86	
	gi 84318929	ribosomal protein L2	6	GVAMNPVDHPHGGGEGR	1687.0	255	158	
	gi 42559303	50S ribosomal protein L2	6			273		
	gi 74312143	acid sensitivity protein	1	GHFFLHPR	1010.5	511	79	
	gi 74314474	elongation factor Ef-Tu	2	AGENVGVLLR	1027.5	394	90	
	gi 74311616	lipid A biosynthesis lauroyl acyltransferase	2	FSTALLHPR	1041.5	306	78	
<i>S. sonnei</i>	gi 74312060	putative outer membrane porin protein	2	RADKPSAGAGR	1085.6	436	89	
	gi 74311030	nitrogen regulatory protein P-II 2	8	QKGHAELYR	1101.2	112	77	
	gi 74314478	50S ribosomal protein L1	5	VVGQLGQVLGPR	1222.6	234	91	
	gi 74311647	23S rRNA pseudouridylyl synthase C	4	LDRDTSGVLLIAK	1400.7	319	102	
	gi 74313409	diaminopimelate decarboxylase	3	FAQKACSNHILR	1500.7	420	85	
	gi 74313634	L-asparaginase II	4	YGFVASGTLNPQKAR	1608.3	348	130	
	gi 74314474	elongation factor Ef-Tu	3	MVVTLIHPIAMDDGLR	1780.3	394	121	
	<i>K. pneumoniae</i>	gi 3954959	nitrogen regulatory protein P-II 2	8	QKGHAELYR	1101.1	112	89
		gi 152972212	50S ribosomal protein L6	6	HADNALTFGPR	1198.2	177	112
		gi 152969641	50S ribosomal protein L32	17	HHITADGFYR	1216.6	57	107
		gi 152972841	50S ribosomal protein L1	5	VVGQLGQVLGPR	1222.5	234	80
		gi 152971771	diaminopimelate decarboxylase	3	FAQKACSNHILR	1500.4	420	85
gi 152968741		pullulanase D protein	2	SALPGSMVANVADER	1615.9	657	157	
gi 7246031		pulD	2			660		
gi 152972232		elongation factor Ef-Tu	4	MVVTLIHPIAMDDGLR	1780.3	394	134	

## RESULTS AND DISCUSSION

We suspected that titania-coated magnetic NPs would have the ability to interact with the phosphate units on the cell walls of Gram-negative bacteria, such as *E. coli*, because LPS, which

contains phosphate units, is a major component of these outer membranes.<sup>28</sup> All Gram-positive bacteria, except *L. monocytogenes*,<sup>29</sup> lack the LPS-like structure, so we expected their interactions with the NPs to be weaker. We employed five

**Table 3. Number of Exact Matches from Peptide Sequence Searches**

MH <sup>+</sup>	peptide sequence	protein	total matches	proteobacteria matches
1010	GHFFLHPR	amino acid antiporter or probable glutamate/ $\gamma$ -aminobutyrate antiporter or acid sensitivity protein	11	11
1027	AGENVGVLLR	elongation factor Ef-Tu or translation elongation factor Tu	98	95
1041	FSTALLHPR	lipid A biosynthesis lauroyl acyltransferase	9	9
1085	RADKPSAGAR	membrane-associated protein or hypothetical protein or putative outer membrane porin protein	18	18
1101	QKGHAELYR	nitrogen regulatory protein P-II 2	31	31
1151	MQFVMRLAR	putative minor tail protein	3	3
1198	HADNALTFGPR	50S ribosomal protein L6	5	5
1216	HHITADGFYR	50S ribosomal protein L32	6	6
1222	VVGQLGQVLGPR	50S ribosomal protein L1	26	26
1230	RVEAEVEAEAK	major outer membrane protein OprF precursor or outer membrane protein and related peptidoglycan-associated (lipo)proteins	2	2
1318	MDITKILNTNR	putative phosphotransferase system (PTS), fructose-specific	2	2
1382	GWLPVVCINPER	hypothetical protein	3	3
1400	LDRDTSGVLLIAK	23S rRNA pseudouridylyl synthase C	4	4
1405	KVSLYLNNETPAG	hypothetical protein	2	2
1406	DVLVNEYGVVEGRR	major outer membrane protein OprF precursor or outer membrane protein and related peptidoglycan-associated (lipo)proteins	3	3
1464	IGFFNPVATGGVEVR	30S ribosomal protein S16	2	2
1500	FAQKACSNIHILR	diaminopimelate decarboxylase	33	32
1608	YGFVASGTLNPQKAR	L-asparaginase II	28	27
1615	SALPGSMVANVVADER	pullulanase D protein or pulD	2	2
1625	MQFYSTPGAGAIRAR	hypothetical protein YfaP precursor	3	3
1687	GVAMNPVDHPHGGGEGR	ribosomal protein L2 or 50S ribosomal protein L2	130	97
1780	MVVTLIHPIAMDDGLR	elongation factor Ef-Tu or translation elongation factor Tu	33	31

Gram-negative bacteria—*E. coli* O157:H7, *P. aeruginosa*, *E. coli* UTI, *S. sonnei*, and *K. pneumoniae*—and three Gram-positive bacteria—*L. monocytogenes*, *S. saprophyticus*, and *S. aureus*—as models to examine their affinity toward Fe<sub>3</sub>O<sub>4</sub>@TiO<sub>2</sub> NPs. Figure 1 displays the capture capacities of the NPs toward these eight bacterial strains. The bacteria were captured under microwave heating for only 1.5 min. Gratifyingly, the Fe<sub>3</sub>O<sub>4</sub>@TiO<sub>2</sub> NPs exhibited much higher capture capacities—by ~1 order of magnitude—toward the Gram-negative bacteria and *L. monocytogenes* than they did toward *S. saprophyticus* and *S. aureus*, which lack the LPS-like structure.

To confirm the mechanism of the interaction between the NPs and the bacterial samples, we employed the Fe<sub>3</sub>O<sub>4</sub>@TiO<sub>2</sub> NPs as affinity probes for LPS. Figure 2a reveals that a series of ions appears at  $m/z < 1400$  in the direct MALDI mass spectrum of LPS (100  $\mu\text{g/mL}$ , 1  $\mu\text{L}$ ). Several of these ions were derived from phosphorylated molecules; for example, the peak at  $m/z$  1038.19 and its fragment ion at  $m/z$  958.55 differ by loss of an HPO<sub>3</sub><sup>-</sup> unit, as do the peak at  $m/z$  998.69 and its fragment at  $m/z$  918.74. Because we added acid during the sample preparation procedure, the signals appearing in the low-mass region were probably derived from the hydrolysis products of LPS. When we decreased the concentration of LPS by 2 orders of magnitude (1  $\mu\text{g/mL}$ , 1  $\mu\text{L}$ ), we observed no ions in the MALDI mass spectrum (Figure 2b). Nevertheless, the peaks that appeared in Figure 2a were evident in the MALDI mass spectrum (Figure 2c) obtained after using the Fe<sub>3</sub>O<sub>4</sub>@TiO<sub>2</sub> NPs to concentrate the target species from this low-concentration LPS (1  $\mu\text{g/mL}$ , 200  $\mu\text{L}$ ). Figure 2d displays the MALDI mass spectrum obtained after using the Fe<sub>3</sub>O<sub>4</sub>@SiO<sub>2</sub> NPs as affinity probes to concentrate the target species from the

same sample containing LPS as that used to obtain Figure 2c; we observe no ions in the mass spectrum. These results imply that phosphorylated molecules interact strongly with the NPs coated with titania and explain why the Fe<sub>3</sub>O<sub>4</sub>@TiO<sub>2</sub> NPs interact with the bacteria that present LPS.

We further employed microwave-assisted affinity capture and tryptic digestion to the bacteria trapped by the Fe<sub>3</sub>O<sub>4</sub>@TiO<sub>2</sub> NPs. Panels a–e of Figure 3 display the MALDI mass spectra obtained after using the Fe<sub>3</sub>O<sub>4</sub>@TiO<sub>2</sub> NPs as affinity probes to trap target bacteria from sample solutions (10  $\mu\text{L}$ ) containing *E. coli* O157:H7 ( $1.8 \times 10^7$  cells/mL), *E. coli* UTI ( $1.3 \times 10^7$  cells/mL), *P. aeruginosa* ( $1.4 \times 10^7$  cells/mL), *S. sonnei* ( $1.9 \times 10^7$  cells/mL), and *K. pneumoniae* ( $1.8 \times 10^7$  cells/mL), respectively, under microwave heating for 1.5 min, followed by on-particle tryptic digestion under microwave heating for another 1 min. We then employed MALDI TOF MS/MS combined with protein database searching to identify peptide sequences for the peaks between  $m/z$  1000 and 2500 derived from each sample. Table 1 lists the corresponding peptide sequences for these peaks that we matched to the five Gram-negative bacteria; for each mass spectrum of Figure 3, Table 2 summarizes the peaks and their corresponding proteins. The details of the MS/MS mass spectra for each peak are provided in the Supporting Information. In Table 1, the peaks at  $m/z$  1010 derived from *E. coli* UTI, *E. coli* O157:H7, and *S. sonnei* may have originated from an amino acid antiporter, the probable glutamate/ $\gamma$ -aminobutyrate antiporter, and an acid-sensitive protein, respectively. Additionally, the peptide sequence appearing at  $m/z$  1010, 1027, 1041, 1085, 1101, 1151, 1222, 1500, and 1780 exists in more than one bacterial strain. Nevertheless, we observed two or three unique signals for each of the five

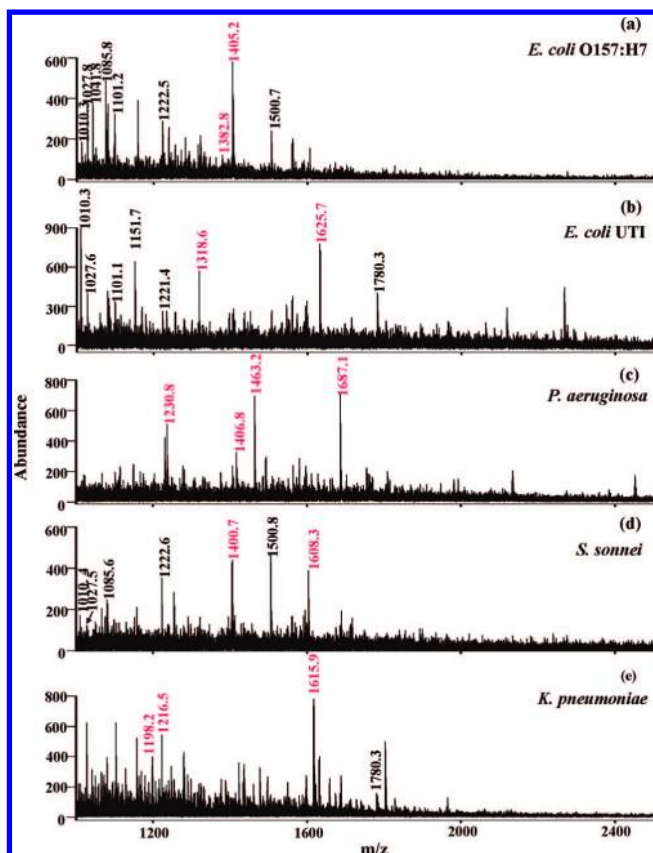


**Figure 4.** MALDI mass spectra obtained after using the  $\text{Fe}_3\text{O}_4@\text{TiO}_2$  NPs (25  $\mu\text{g}$ ) as affinity probes to trap target bacteria from aqueous samples (10  $\mu\text{L}$ ) containing (a) *E. coli* O157:H7 ( $3.70 \times 10^4$  cells/mL), (b) *E. coli* UTI ( $2.64 \times 10^4$  cells/mL), (c) *P. aeruginosa* ( $2.89 \times 10^4$  cells/mL), (d) *S. sonnei* ( $3.81 \times 10^4$  cells/mL), and (e) *K. pneumoniae* ( $3.64 \times 10^4$  cells/mL) under microwave heating (power, 900 W) for 1.5 min, followed by on-particle tryptic digestion under microwave heating (power, 900 W) for 1 min. CHCA (25 mg/mL, 1  $\mu\text{L}$ ) was the MALDI matrix.

bacterial strains—at  $m/z$  1198 (*K. pneumoniae*), 1216 (*K. pneumoniae*), 1230 (*P. aeruginosa*), 1318 (*E. coli* UTI), 1382 (*E. coli* O157:H7), 1400 (*S. sonnei*), 1405 (*E. coli* O157:H7), 1406 (*P. aeruginosa*), 1464 (*P. aeruginosa*), 1608 (*S. sonnei*), 1615 (*K. pneumoniae*), 1625 (*E. coli* UTI), and 1687 (*P. aeruginosa*)—that could be used as potential biomarkers. Furthermore, it is interesting that *E. coli* O157:H7 and *E. coli* UTI have unique biomarker ions even though they differ only at the level of the strain. For example, the peak at  $m/z$  1085, which is derived from a membrane-associated protein (43–53, RADKPSAGAGR), appears only in the MALDI mass spectrum of *E. coli* O157:H7. We utilized BLAST to search for this protein in *E. coli* UTI. Interestingly, the protein is mutated in *E. coli* UTI: amino acid 51 of the protein sequence has been mutated from alanine to threonine (see Supporting Information). This mutation accounts for why the peak at  $m/z$  1085 is missing in the MALDI mass spectrum of *E. coli* UTI (Figure 3b). These results suggest the possibility of using this approach to differentiate between bacterial strains. We note, however, that the peak at  $m/z$  1085, which is derived from the putative outer membrane porin protein, also appears in the MALDI mass spectrum of the tryptic digest of *S. sonnei*. Nevertheless, we can still differentiate *E. coli* UTI, *E. coli* O157:H7, and *S. sonnei* by their unique biomarker ions at  $m/z$  1318 and 1625,  $m/z$  1382 and 1405, and

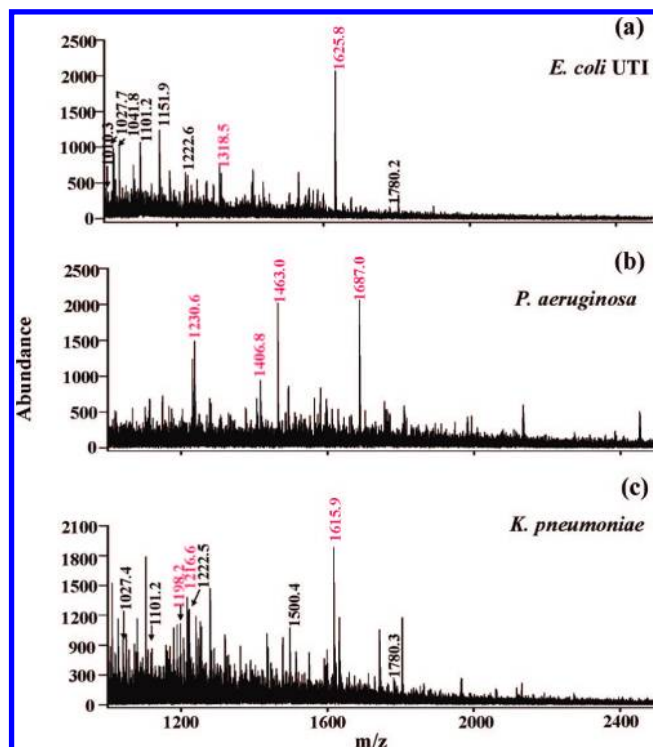


**Figure 5.** MALDI mass spectra obtained after using the  $\text{Fe}_3\text{O}_4@\text{TiO}_2$  NPs (25  $\mu\text{g}$ ) as affinity probes to trap target bacteria from urine samples (10  $\mu\text{L}$ ) containing (a) *E. coli* UTI ( $6.60 \times 10^5$  cells/mL), (b) *P. aeruginosa* ( $7.21 \times 10^5$  cells/mL), and (c) *K. pneumoniae* ( $9.14 \times 10^5$  cells/mL) under microwave heating (power, 900 W) for 1.5 min, followed by on-particle tryptic digestion under microwave heating (power, 900 W) for 1 min. CHCA (25 mg/mL, 1  $\mu\text{L}$ ) was the MALDI matrix.

$m/z$  1400 and 1608, respectively. In addition, when utilizing BLAST to search for corresponding proteins that provide ions at  $m/z$  1230, we obtained two proteobacterial matches. Fortunately, both of these proteins originate from *P. aeruginosa*. Furthermore, although there are three matches for the ion at  $m/z$  1406, again these proteins all originate from *P. aeruginosa*. That is, the ions at  $m/z$  1230 and 1406 are potential biomarkers for *P. aeruginosa*. BLAST searching also revealed that the ions at  $m/z$  1405 and 1615 exist only in *E. coli* O157:H7 and *K. pneumoniae*, respectively (Table 3). However, because the current databases of bacterial genome sequences are incomplete, the statement is only valid when the discussion is limited to these five bacterial strains. Additionally, these resulting ions derived from the tryptic digests of these bacteria did not appear in the MALDI mass spectra when the tryptic digestion of bacteria was carried out under microwave heating for 1 min in the absence of magnetic iron oxide nanoparticles (see Supporting Information). The results indicate that the presence of magnetic nanoparticles in the digestion solutions indeed accelerate the tryptic digestion of bacteria.

Next, we examined the detection limits of this approach. Panels a–e in Figure 4 display the MALDI mass spectra obtained after using the  $\text{Fe}_3\text{O}_4@\text{TiO}_2$  NPs as affinity probes to trap target bacteria from sample solutions (10  $\mu\text{L}$ ) containing *E. coli* O157:H7 ( $3.7 \times 10^4$  cells/mL), *E. coli* UTI ( $2.6 \times 10^4$  cells/mL), *P. aeruginosa* ( $2.9 \times 10^4$  cells/mL), *S. sonnei* ( $3.8 \times 10^4$  cells/mL), and *K. pneumoniae* ( $3.6 \times 10^4$  cells/mL), respectively, under microwave heating for 1.5 min, followed by on-particle tryptic digestion under microwave heating for another 1 min. The potential biomarker ions represent-



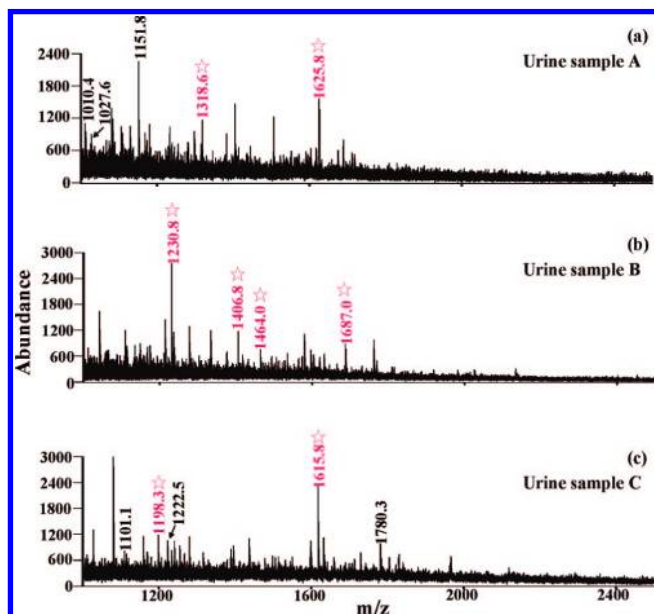


**Figure 6.** MALDI mass spectra obtained after using the  $\text{Fe}_3\text{O}_4@ \text{TiO}_2$  NPs (25  $\mu\text{g}$ ) as affinity probes to trap target bacteria from clinical urine samples (a) A, (b) B, and (c) C, which contained *E. coli* UTI, *P. aeruginosa*, and *K. pneumoniae*, respectively, under microwave heating (power, 900 W) for 1.5 min, followed by on-particle tryptic digestion under microwave heating (power, 900 W) for 1 min. CHCA (25 mg/mL, 2  $\mu\text{L}$ ) was the MALDI matrix. Potential biomarker ions were marked with asterisks.

ing each bacterial strain summarized in Figure 3 and Table 2 are still present in the MALDI mass spectra obtained from these low-cell-concentration bacterial samples. The detection limits for the five bacteria when employing this approach were as low as  $\sim 10^4$  cells/mL; sample solution volumes as low as 10  $\mu\text{L}$  were sufficient to perform the analyses. Thus, only several hundred bacterial cells are required for characterization using this new approach.

Next, we further searched the peptide sequences listed in Table 1 against the sequences of all proteins in the nonredundant protein sequence database using BLAST. Table 3 lists the search results. The ions at  $m/z$  1027, 1500, 1608, 1687, and 1780 can be found in nonproteobacterial strains, but the rest of the ions only appear in proteobacterial strains. These ions are derived from either outer membrane proteins or ribosome proteins. Our findings suggest that this approach can provide potential biomarker ions derived not only from the cell walls but also from the interior of bacterial samples.

To examine the effectiveness of this approach in a real-world application, we analyzed urine samples spiked with bacteria. Panels a–c in Figure 5 display the MALDI mass spectra obtained after using the  $\text{Fe}_3\text{O}_4@ \text{TiO}_2$  NPs as affinity probes to trap target bacteria from urine samples (10  $\mu\text{L}$ ) containing *E. coli* UTI ( $6.60 \times 10^5$  cells/mL), *P. aeruginosa* ( $7.21 \times 10^5$  cells/mL), and *K. pneumoniae* ( $9.14 \times 10^5$  cells/mL), respectively, under microwave heating for 1.5 min, followed by on-particle tryptic digestion under microwave heating for 1 min. The biomarker ions at  $m/z$  1318.5 and 1625.8, which represent *E. coli* UTI, appear in the mass spectrum in Figure 5a; biomarker ions at  $m/z$  1230.6, 1406.8, 1464.0, and 1687.0, which represent *P. aeruginosa*, appear in Figure 5b; biomarker ions at  $m/z$  1198.2, 1216.6, and 1615.9, which represent *K. pneumoniae*,

appear in Figure 5c. These results indicate that this new approach can be used to rapidly characterize trace levels of bacteria, even in complex urine samples. The detection limit when employing this approach to characterize bacteria from urine samples is as low as several hundred bacterial cells, similar to that obtained from aqueous samples (see Supporting Information for details). Furthermore, we also repeatedly performed the experiment and found the potential biomarker ions reproducibly appear in the mass spectra (see Supporting Information). The results show high promise of the effectiveness of this approach for rapid identification of trace levels of bacteria.

After demonstrating the feasibility of our approach for urine samples spiked with bacteria, we further employed this approach to the analysis of urine samples directly collected from patients with urinary tract bacterial infections. Panels a–c in Figure 6 display the MALDI mass spectra obtained after using the  $\text{Fe}_3\text{O}_4@ \text{TiO}_2$  NPs as affinity probes to trap target bacteria from the urine samples (15  $\mu\text{L}$ ) labeled A, B, and C containing *E. coli* UTI, *P. aeruginosa*, and *K. pneumoniae*, respectively, under microwave heating for 1.5 min, followed by on-particle tryptic digestion under microwave heating for 1 min. The potential biomarker ions at  $m/z$  1318.6 and 1625.8, which represent *E. coli* UTI, appear in the mass spectrum in Figure 6a; biomarker ions at  $m/z$  1230.8, 1406.8, 1464.0, and 1687.0, which represent *P. aeruginosa*, appear in Figure 6b; biomarker ions at  $m/z$  1198.3 and 1615.8, which represent *K. pneumoniae*, are revealed in Figure 6c. These potential biomarker ions are marked with asterisks. Furthermore, the peaks at  $m/z$  1010.4, 1027.6, and 1151.8 listed in Table 2 are also observed in Figure 6a although they are not only found in the MALDI mass spectra derived from *E. coli* UTI. The peaks at  $m/z$  1101.1, 1222.5, and 1780.3, possibly derived from *K. pneumoniae* (see Table 2), also appear in Figure 6c. Although there are still many other unidentified ions appearing in the mass spectra, the potential biomarker ions representing specific bacterial strains can be readily identified in the mass spectra based on the potential biomarker ions listed in Table 2. The results look quite promising; this approach seems very suitable to be used in characterization of these bacterial strains in clinical samples.

## CONCLUSIONS

We have identified possible biomarkers for five Gram-negative bacterial strains in this study involving  $\text{Fe}_3\text{O}_4@ \text{TiO}_2$  NP-based affinity capture and tryptic digestion under microwave heating. The five bacterial strains are readily differentiated based on these potential biomarker ions. In addition, *E. coli* O157:H7 and *E. coli* UTI, which differ at the strain level, can also be differentiated easily based on current data. To the best of our knowledge, this paper provides the first example of using a NP-based proteomic strategy to successfully differentiate *E. coli* O157:H7 from *E. coli* UTI. The reproducibility of detecting the explored biomarker ions is quite good, and the sensitivity is extremely high. Samples comprising only 200–300 bacterial cells in 10  $\mu\text{L}$  of solution are sufficient for bacterial identification using this approach. When the cell concentrations of the bacterial samples approach their detection limits, the detection of the biomarker ions in their MALDI mass spectra remains reproducible. The greatest advantage of this approach is its

short analysis time (~15 min), which does not require time-consuming bacterial culturing. Furthermore, we have also demonstrated the suitability of using this approach to rapidly characterize bacterial strains from urine samples. Although the  $\text{Fe}_3\text{O}_4@\text{TiO}_2$  NPs have higher affinity toward bacteria containing LPS, such as Gram-negative bacteria, the NPs still interact with Gram-positive bacteria. If Gram-positive bacteria that lack LPS are the dominant species within a sample, the NPs will be capable of concentrating them from sample solutions. Thus, the  $\text{Fe}_3\text{O}_4@\text{TiO}_2$  NPs have broad affinity for bacteria. The main obstacle of this approach for its practical application is that the protein database of bacteria is incomplete. Nevertheless, if the analytical samples contain any or all of the five Gram-negative bacteria presented in this study, this approach can be used to readily identify these bacteria. Because of the short analysis times and reproducibility, we believe that this technique has great potential for applications in rapidly characterizing bacterial

strains, especially when bacteria-related protein databases become more complete.

#### **ACKNOWLEDGMENT**

We thank the National Science Council (NSC) of Taiwan and the MOE-ATU (96W821G021 and 96W801H109) for supporting this research financially. We also thank Prof. Yaw-Kuen Li (NCTU) for lending us the required equipment for bacterial culturing.

#### **SUPPORTING INFORMATION AVAILABLE**

Additional information as noted in text. This material is available free of charge via the Internet at <http://pubs.acs.org>.

Received for review September 26, 2008. Accepted October 27, 2008.

AC802042X